[AMERICAN JOURNAL OF SCIENCE, VOL. 287, DECEMBER, 1987, P. 979–1007]

GEOCHEMICAL SELF-ORGANIZATION I: REACTION-TRANSPORT FEEDBACKS AND MODELING APPROACH*

PETER ORTOLEVA, ENRIQUE MERINO, CRAIG MOORE, and JOHN CHADAM

Geo-Chem Research Associates, 400 East Third Street, Bloomington, Indiana 47401

ABSTRACT. Self-organization is the autonomous passage of a system from an unpatterned to a patterned state without the intervention of an external template. Self-organization requires feedback and disequilibrium, both of which occur in geochemical systems. There are several isothermal reaction-transport feedbacks that can, in principle, produce mineral and textural patterns. Furthermore there exist in rocks of all kinds many cases of chemical, mineral, or textural patterns (such as cement bands, metamorphic layering, oscillatory zoning, and others) that cannot have been inherited, and whose genesis therefore must have involved self-organization. Combined theoretical, experimental, and petrological evidence indicates that geochemical self-organization is widespread in rocks.

Disequilibrium can be imposed on the system through either the initial or the boundary conditions. Some possible reaction-transport feedbacks in geochemical systems are qualitatively described herein, including the reactive-infiltration instability, the supersaturation–nucleation–depletion cycle, autocatalytic crystal growth, and two stress–texture–solubility instabilities. Also described are the textural and mineral patterns that should be brought about by these feedbacks.

These reaction-transport feedbacks and others can be modeled by sets of differential equations that provide for mass conservation, rates of homogeneous reactions and first-order phase transitions, and transport by diffusion, hydrodynamic dispersion, and flow. Because these sets of equations are normally very "stiff" (that is, they contain some terms that are orders of magnitude greater than others), their conventional numerical solution over geologically realistic times and distances would take prohibitively long computing times.

In the modeling we describe here, the very stiffness of the problem becomes the key to its numerical solution. The equations are scaled in terms of "smallness parameters" which express the order-of-magnitude contrast between fast and slow reaction rates and that between typical aqueous concentrations and mineral densities. The behavior of the equations is studied as these smallness parameters tend to zero. This asymptotic analysis permits numerical solutions of the differential equations to be carried out over geologically relevant times and distances. These calculations (examples of which will be given in subsequent papers) yield the values of all relevant descriptive variables (solute concentrations in the intergranular fluid, grain size, modal amounts, porosity) as functions of time and space and can

* Research supported in part by the U.S. Department of Energy, Basic Energy Sciences, Engineering Research Program, Contract #DE-AC02-82ER074.

predict the generation of self-organizational textures and mineral distributions consistent with those observed in nature.

I. INTRODUCTION

Self-organization is the autonomous passage of a system from an unpatterned to a patterned state without the intervention of an external template. One necessary condition for self-organization is that the system be sufficiently far from equilibrium, and another is that at least two processes active in the system be coupled (Nicolis and Prigogine, 1977). Because several types of reaction-transport loops can operate in geochemical systems and because these systems are most often out of equilibrium, geochemical self-organization should be expected to be commonplace.

Interest in the genesis of repetitive, non-inherited mineral patterns in rocks dates back to Knopf (1908), Liesegang (1913, 1915), and Hedges and Myers (1926), who attempted to explain certain mineral bandings as the result of the interdiffusion and coprecipitation of solutes. Later Turing (1952) showed that a uniform chemical system can be unstable to the formation of repetitive patterns of composition through the interaction of reaction and transport.

The aim of this series of papers is to study the phenomenon of geochemical self-organization in reaction-transport systems. In this paper we (A) present textures that demonstrate the ability of many rocks to self-organize; (B) qualitatively discuss several unstable feedback mechanisms that can operate in geochemical systems, as well as the patterns produced by these feedbacks; and (C) set forth a new modeling approach to the dynamics of water-rock interaction that accounts for geochemical self-organization. Future papers in this series will contain detailed quantitative models of reaction-transport feedbacks relevant in weathering, diagenesis, metamorphism, and hydrothermal alteration. The reactive-infiltration instability, which causes a reaction front to become fingered, will be the object of the second article. The supersaturation–nucleation–depletion cycle (which can cause the precipitation of regular bands of authigenic cement) and a pressure solution model of metamorphic differentiation will be treated in later papers of the series.

Many textures in rocks of all kinds contain conclusive evidence that some kind of geochemical self-organization has taken place. Such textures consist of one or another ordered spatial arrangement of minerals or textural features that can be shown, by any combination of field, petrographic, or chemical criteria, not to have been inherited. One good example of this is a set of evenly spaced stylolites that cut across the bedding in a monomineralic rock: the set of stylolites implies the formation of planar pressure-*dissolution* regions that alternate in space with *precipitation* regions. The generation of these regularly alternating regions cannot have been inherited from or in any way predetermined by the sediment, because the regions intersect the stratification. The ordered arrangement of stylolites must have been

produced by some particular interaction among the variables, forces, and mechanisms involved—stress, texture, dissolution, precipitation, and transport. The set of stylolites is thus conclusive evidence of some type of geochemical self-organization. Needless to say, stylolites that coincide with bedding planes are more difficult to prove to be non-inherited or not predetermined by some sedimentological textural feature.

Other good self-organization textures are alternatingly layered orbicules in igneous rocks and alternatingly banded concretions in sedimentary rocks; in both cases the very body that contains the repeated mineral bands has formed *in-situ* and is thus non-inherited. Still other conclusive and conspicuous examples of one or another kind of geochemical self-organizations, such as metamorphic layering, oscillatory zoning, and stratification-crossing banded cements, are listed, in table 1 (p. 982). These examples suggest that self-organization can take place in rocks of all types: sedimentary, metamorphic, and igneous. One would expect that these phenomena have different mechanistic origins. Some of these are discussed in section III.

II. GENERAL PRINCIPLES

A theory of self-organization consists of several elements that are useful in other fields but that may not be entirely familiar to the reader. In this section we delineate these concepts and set forth a general approach that allows for the formulation of a set of equations giving the spatio-temporal behavior of the relevant descriptive variables. With these equations one may quantitatively predict geochemical conditions favorable for self-organization.

A. Descriptive Variables

The examples of the previous section indicate that repetitive patterns observed in rocks involve the spatial variation of a number of macroscopic quantities. In general, descriptive variables that can become patterned include:

1. Solute concentrations in pore fluids
2. Adsorbate concentration on grain surfaces
3. Grain shape, volume, crystallographic orientation, composition, defect density, and number density (grains/rock volume)
4. Porosity and permeability of the rock
5. Pressure and temperature
6. Isotopic concentrations in pore fluids or mineral grains
7. Pore fluid or rock plastic flow velocity
8. Microbe population density

Items 3 and 4 are variables that must be specified for all minerals to describe the texture of a rock. The implication of this list of variables is that self-organization may, in principle, take place with respect to many quantities.

TABLE 1

List of geochemical self-organization phenomena

1. Oscillatory zoning in plagioclase crystals	Smith, 1974
2. Repetitive layers in igneous intrusions	McBirney and Noyes, 1979 Boudreau, 1984
3. Orbicules	Leveson, 1966 Moore, 1984
4. Metamorphic differentiation	Hobbs, Means, and Williams, 1976 Orville, 1969 Turner and Weiss, 1963 Vidale, 1974 Ortoleva, Merino, and Strickhom, 1982
5. Banded skarns	Jahns, 1944 Guy, 1981 Kwak and Askins, 1981 Williams, Turner, and Gilbert, 1982 Gower, Clark, and Hodgson, 1985
6. Clots and orbicules in contact metamorphic aureoles	Tolok and Fedchin, 1970 Hosking, 1953–54 Moore, unpub. Knopf, 1908 Tanelli 1982 Patterson, Ohmoto, and Solomon, 1981 Salomon, 1894
7. Stylolites and pressure solution seams	Barrett, 1964 Dunnington, 1967 Tremolieres and Reulet, 1978 Simpson, 1985 Spang, Oldershaw, and Stout, 1979 Merino, Ortoleva, and Strickholm, 1983
8. Repetitive patterns of iron oxide cement	Hobson, 1930 Merino, 1984 DeCelles and Gutschick, 1983 Hereford, personal commun., 1980 Bailey and Childers, 1977 Merino, in preparation
9. Banded agates	Liesegang, 1915 Frondel, 1978, 1982, 1985 Merino, 1984
10. Iron-rich and iron-poor mineral bands	Trendall, 1972 Hartman and Dickey, 1932 Grubb, 1971 Mel'nik, 1982
11. Banding in Mississippi Valley-type ores	Beales and Hardy, 1980 Fontbote and Amstutz, 1982
12. Reaction front scalloping	Galloway, 1978 Boeglin, 1981 Ortoleva and others, 1986a Moore, unpub. Nahon, personal commun.

B. Processes

Delineating the processes operative in a given situation is key to uncovering the types of self-organization that are possible. The list is quite long, suggesting the potential variety of geochemical self-organization phenomena.

1. Homogeneous reactions among solute species
2. Adsorption/desorption at grain surfaces

3. Grain nucleation, growth, replacement, and dissolution
4. Creation and destruction of grain defects
5. Isotope exchange
6. Microbe metabolic, reproductive, and other biochemical reactions
7. Diffusion, dispersion, and thermal conduction
8. Percolation, advection
9. Electrically driven ion migration
10. Microbe migration

These processes may be divided into two types—local and transport. In the context of self-organization they play fundamental and complementary roles. Local processes (items 1–6) allow for variations within a given volume element of the descriptive variables due to exchange of mass among minerals, solutes, and biological species. Transport processes (items 7–10), on the other hand, allow for exchange of matter and energy between volume elements and, therefore, are required to create the spatial redistribution of the descriptive variables constituting the pattern.

C. Dynamical Equations

In each specific case of self-organization typically a few processes determine the form of the dynamical equations that yield the spatial development of the descriptive variables. The relevant equations may be derived from the conditions of conservation of mass, energy, and momentum (DeGroot and Mazur, 1962). For electrical phenomena (as in supergene enrichment of some metals), Poisson's equation for the electrical potential must also be invoked. While the specific form of the conservation equations depends strongly on the operative processes, in general they are partial differential equations that express the rate of change of a descriptive variable as a sum of terms, one for each individual process: for a descriptive variable ψ we write

$$\frac{\partial \psi}{\partial t} = \sum_{\substack{\text{process} \\ \#i}} \left[\frac{\partial \psi}{\partial t}\right]_i$$

where $(\partial\psi/\partial t)_i$ represents the contribution that process i makes to the total rate of change of ψ, $(\partial\psi/\partial t)$ at a given point. These contributions involve various spatial derivatives from the transport laws and depend not only on ψ but on other descriptive variables; it is this latter feature that allows for the coupling necessary for geochemical self-organization.

D. Boundary Conditions, Initial Data, and Disequilibrium

To solve the equations for the spatio-temporal evolution of the descriptive variables we need first to define the spatial extent of what we call the "system" and the rest of the universe, or "environment." This distinction is often not obvious and is sometimes a matter of convenience

or mathematical simplicity. In any case, the system is the domain wherein the phenomenon of interest takes place. The mathematical surface separating the system from the environment is called the boundary, and it is through the boundary that the system communicates with the environment. The mathematical statements quantifying that interaction are the "boundary conditions." The "initial data" are the spatial distributions of the descriptive variables at the initial instant.

As displacement from equilibrium is a necessary condition for self-organization, we now turn to the question of how the system may be driven out of equilibrium. In setting forth situations that can drive a geochemical system out of equilibrium we take a first step toward understanding the specific geochemical contexts in which self-organization may take place. Disequilibrium is dictated by the initial data and the boundary conditions. To illustrate how each of these two factors may specify disequilibrium, we consider two idealized situations borrowed from chemical engineering and indicate geochemical analogues.

1. Batch mode.—"Batch mode" chemical processing is carried out by placing reactants in a vessel and allowing the reaction to proceed until a sufficient yield of a desired product is produced. In batch mode the relevant processes start off because the initial composition is not at equilibrium. In principle, batch mode could also be carried out by adding the constituents at equilibrium at a given pressure and temperature and then changing the latter parameters at the initial instant. In either case it is clear that a *batch mode system is driven transiently out of equilibrium through the initial data.* An example is the Zhabotinsky reaction, a classical experimental case of chemical self-organization (Field and Berger, 1985, and citations therein). A geological example of batch mode disequilibration would be a magma body injected from depth into a host rock at a lower pressure and temperature and subsequent isochemical cooling. Another possible example of "batch-mode" disequilibrium is that of a rock under an overall stress, though here no exchange of matter need take place with the environment. The stress drives the system out of equilibrium and causes dissolution and precipitation either through pressure solution or through creation of lattice defects. Mechanical energy is supplied from the environment, and the heat generated is conducted out.

2. Exchange mode.—Here the system is pushed, and kept, out of equilibrium by continuous exchange of reactants and products with outside, "constant-composition reservoirs." In this type, the disequilibrium is imposed on the system through the boundary conditions.

Geological displacement from equilibrium can occur in many ways. The ultimate driving forces for disequilibrium are heat flow from the Earth's interior, solar radiation, loss of energy to free space, and applied gravitational stresses, but it is more instructive in unraveling self-organization phenomena to analyze smaller scale processes.

Consider the following examples of exchange-mode disequilibrium, chosen to illustrate the wide variety of conditions under which

geochemical self-organization can take place. One is an aquifer into which water is continuously injected which is out of equilibrium with some of the minerals in the rock constituting the system. A moving reaction zone is set up. As the water flows through it, it reacts with the initial minerals and thereby becomes equilibrated with them. Thus, within the reaction zone mineral dissolution and precipitation are maintained out of equilibrium. Similar cases of continuous flow through systems are thermo-convective cells, compaction flows, and hydrothermally driven liquid and vapor flows. Engineered geochemical reaction fronts include acidification fronts in secondary oil recovery, flame fronts in *in situ* coal gasification, and dissolution fronts in leach mining.

E. Autonomy, Noise, and Self-Organization

As mentioned in the introduction, the periodic patterning that constitutes self-organization arises autonomously and does not require externally applied periodic causes. If they existed, these periodic causes would manifest themselves in the initial data or boundary conditions.

Noise can be fundamental in triggering self-organization. Noise can exist in the initial data, in the boundary conditions, and in the rates of the processes that operate in the system. 'Noise' describes all the random deviations of a variable from an average value and in a sense contains aspects of all possible patterns. Self-organization can be thought of as the ability of a system to select one pattern from all possible noise-generated patterns and amplify it into a well-ordered observable structure. The texture of any rock always contains deviations from perfect uniformity. It is these small deviations that are first enlarged by feedback loops; then some set of deviations increases faster than the others also present in the initial noise and dominates them. We now discuss examples of feedback loops in geochemical systems.

III. GEOCHEMICAL FEEDBACK

A *positive* feedback loop is a sequence of processes that is closed on itself; each process promotes itself through the others in the loop (that is, A promotes B which in turn promotes C which then promotes A, et cetera). In contrast, a *negative* feedback loop is typified by the sequence: A promotes B which in turn promotes C, which tends to suppress A, et cetera. A negative feedback loop with time delays can induce temporal oscillatory order. We now give geochemical examples of these two types of loops and discuss how they can drive self-organization.

A. Reactive Infiltration Feedback

When water flows through a porous rock and reacts with one or more of its minerals, a reaction zone or front is established that slowly advances downflow and that separates the altered region (upflow from the front) from the still-unaltered region (downflow from it). In the altered region the authigenic mineralization is determined ultimately by the composition of the incoming fluid. By contrast, the unaltered region

is the rock-dominated zone, and the aqueous solutions in it are in equilibrium with the original mineralogy. The inlet fluid composition is transformed into that in the rock-dominated zone as the fluid passes through the reaction zone. This advancing reaction zone is, by its very nature, out of equilibrium and has the potential to drive self-organization.

Consider a small region of rock in the reaction zone and assume that the porosity is slightly larger in that small region than elsewhere. Then, often, the local permeability will also be larger there and, by Darcy's law, so will the discharge of reactive water through that small region. This faster flow will cause faster local dissolution, which in turn will again increase the local porosity and permeability, completing a positive feedback loop. The feedback can be represented by two tubes (fig. 1), both feeding from a common source and both containing a porous rock, with some minerals soluble in the water. If the dissolution front gets slightly more advanced in one tube, I, than in other, II, then more of the flow goes through I, because its overall permability becomes larger—"overall permeability" being defined as the net flow-through per unit overall pressure gradient across the tube. As shown in figure 1, the increased discharge through I advances the front even farther ahead in I than in II. A key step in the loop, as shown also in figure 2, is that the increased flow in channel I is captured from channel II due to the larger overall permeability of the medium in I.

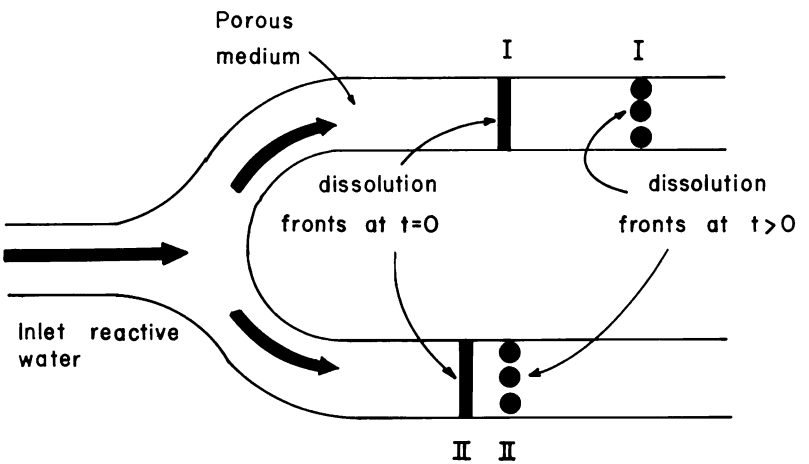

Fig. 1. A schematic reaction-advection system consisting of two parallel channels. The two channels have roughly the same initial porosity and permeability and are connected at their inlet end so that the one with the slightly higher overall permeability will capture flow from the other at the inlet. The net pressure difference across each is taken to be the same. Since the inlet waters are out of equilibrium with at least one of the minerals in the channels, dissolution fronts advance down both channels. But, because the influx of reactive water through I is greater than through II, the front in I moves faster than through II no matter how little the I front was initially ahead of the II front.

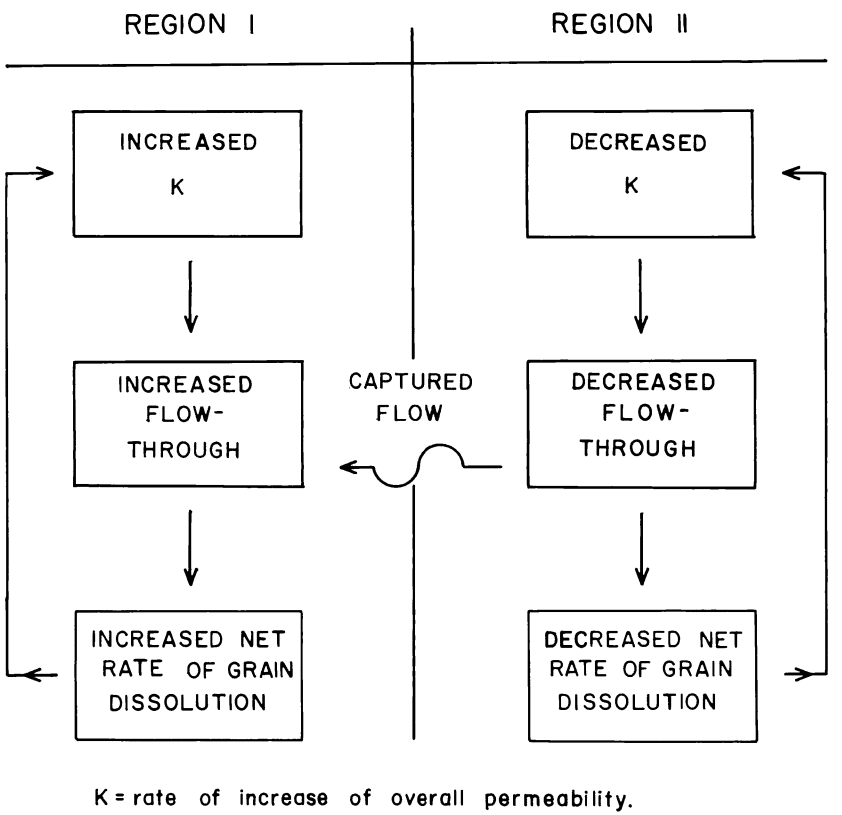

Fig. 2. Feedback loop for the reaction-infiltration instability between channels I and II of figure 1. The "overall permeability" is defined as the ratio of the flow-through velocity to the overall pressure difference. The cross coupling of channels through the captured flow is an essential part of the feedback loop.

The spontaneous fingering of the front constitutes a morphological self-organization sustained by focused flow, as shown in figure 3. The fingers developed by the reaction front as it sweeps through the rock increase progressively in length but only up to a limit. The longer a finger becomes, the longer the water reaching its tip has had to pick up solutes by diffusion from the sides. Hence the fluids reaching the tip are increasingly equilibrated, as the finger length-to-width ratio increases. This phenomenon prevents fingers from growing indefinitely and forces them to reach a given length-to-width ratio dictated by the system parameters (composition of the inlet water, imposed rate of flow, and composition of the unaltered rock). The above mediating effect (along with two-channel-like competition for total flow-through) also acts to repress a periodic array of fingers (scalloping) when the wavelength is too small.

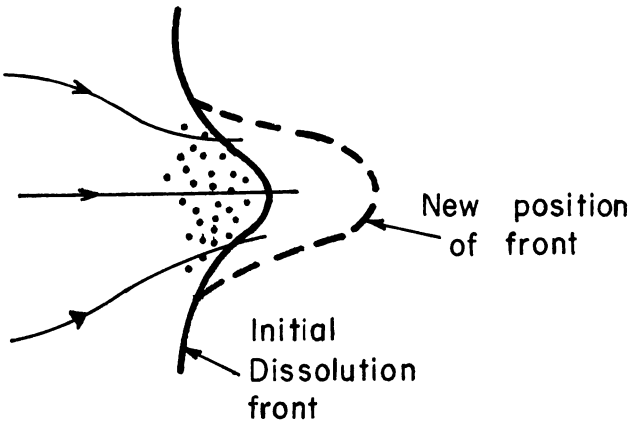

Fig. 3. The feedback loop of figure 2 can also operate in a continuous mode, as opposed to the discrete, two-channel model of figure 1. The transverse components of the flow focus reactive waters toward the tip of the growing and advancing bump in the dissolution front. The front is depicted here as being sharp, although real fronts are gradational on some scale. The slightly higher-porosity regions (stippled, corresponding to a local nonuniformity in rock texture) at the bumps attract and focus the flow of reactive water. This captured flow pushes the bumps in the front forward (dashed), tending to make them more elongate.

The reactive-infiltration feedback is probably responsible for the scalloped reaction fronts and textures described in the Introduction (example 12) and will be the subject of a detailed modeling study in the second article of this series.

B. The Supersaturation-Nucleation-Depletion Cycle

Spatially periodic structures may also result from negative feedback. In the present case the negative feedback involves repression of nucleation at one point in space caused by nucleation and particle growth at a neighboring point. Consider the influx of X-charged water into a rock containing disseminated grains of a mineral A. Assume that the schematic coupled reactions

$$X + A \rightleftharpoons Y$$
$$X + Y \rightleftharpoons B$$

take place, with X and Y being aqueous species, and B a product mineral. If this process is driven by an influx of X-laden water then the precipitation of mineral B in an initially B-free rock can be banded. The bands of cement arise as follows (see fig. 4). Nucleation and growth of B at one point (call it point I) consume X and Y, so that their concentration product falls below its critical value for B supersaturation for nucleation. Therefore, nucleation downstream from I can be repressed, if B growth at I is sufficiently fast. However, as the A-dissolution front moves

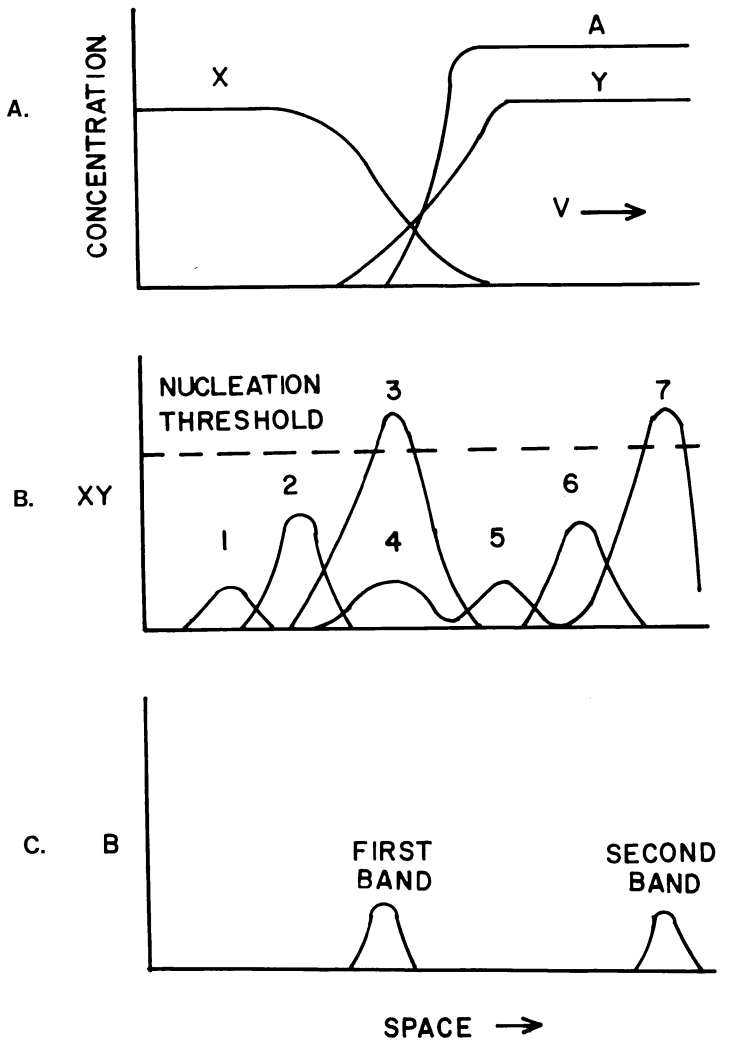

Fig. 4. The Ostwald-Liesegang cycle for the processes of subsection III.A.2. Shown are the schematic profiles of concentrations (moles/rock volume) of aqueous and mineral species. The system, initially with mineral A only, is subjected to a flow of X-rich fluids of velocity v and direction as indicated by the arrow. This leads to the dissolution front of Frame **A.** When the concentration product XY exceeds a critical supersaturation value as at time 3 in Frame **B**, nucleation of B takes place. By upstream diffusion, the growth of B attracts and consumes Y from the A-dissolution front further downstream (as seen in the decrease in XY from time 3 to time 4) and thus represses nucleation farther downstream. When the A-dissolution front proceeds sufficiently far downstream from the first nucleated B band, a second B band can be nucleated (see Frame **C**) because upstream Y diffusion is no longer effective in reducing the XY product as shown by the profiles at times 5 to 7 of Frame **B.**

sufficiently far downstream from I, upstream diffusion of the Y produced at the front becomes negligible, eventually stopping B growth at I and allowing new nucleation of B at the current position of the A front. Repetition of this sequence of events constitutes the Ostwald-Liesegang cycle of supersaturation-nucleation-depletion shown schematically in figure 4. It is convenient to think of the "system" as the vicinity of the A dissolution front. Thus X-rich waters continuously enter the system and A-equilibrated waters continuously exit. The B that precipitates is also lost from the system. Thus, B nucleated at an earlier time represses nucleation in the (moving) system at a later time. This is an example of a time-delayed, negative feedback oscillation. Ortoleva (1984a, b) and Ortoleva and others (1986a) invoked this mechanism to explain iron oxide banding associated with uranium roll-type deposits and other redox-fronts. A detailed modeling study of this negative feedback will be presented in a future article in this series.

C. Autocatalytic Surface Attachment

A mixed positive and negative feedback is probably the cause of oscillatory zoning of albite and anorthite in plagioclases of intermediate igneous rocks. For illustrative purposes, we analyze an A-B solid solution growing from A and B units in a melt.

Consider the possibility that, because of lattice strains, chemical bonding, geometric packing preferences, or purely kinetic effects, the precipitation of A units on an A-rich grain surface is much faster than precipitation of B on an A-rich surface. This promotion of A precipitation by A already precipitated is a type of autocatalysis. As autocatalytic A precipitation progresses, however, the melt in the vicinity of the growing grain becomes depleted in A. Eventually A can become so depleted in the melt because of preferred A incorporation on an A-rich crystal surface that B becomes concentrated enough in the melt to force growth of B-rich layers. If B growth is also autocatalytic the grain can get locked into a B-rich growth phase for a period until A buildup by diffusion to the vicinity of the grain surface from farther out in the melt (plus depletion of B by growth of B-layers) becomes sufficiently large that A growth can once again start, completing the cycle. This is shown schematically in figure 5. As in the Ostwald-Liesegang feedback loop, time delay and repression play key roles in the oscillation. The present autocatalytic nature of the A and B incorporation rates increases the potential for oscillatory behavior. The phenomenon has been quantitatively modeled by Haase and others (1980); see also Simakin (1983) and references therein.

D. Mechano-Chemical Feedback in Stressed Rocks

A host of self-organization feedback loops may operate in stressed rocks. The overall stress can induce mineral dissolution or nucleation and growth, thus producing the displacement from chemical equilibrium necessary for self-organization.

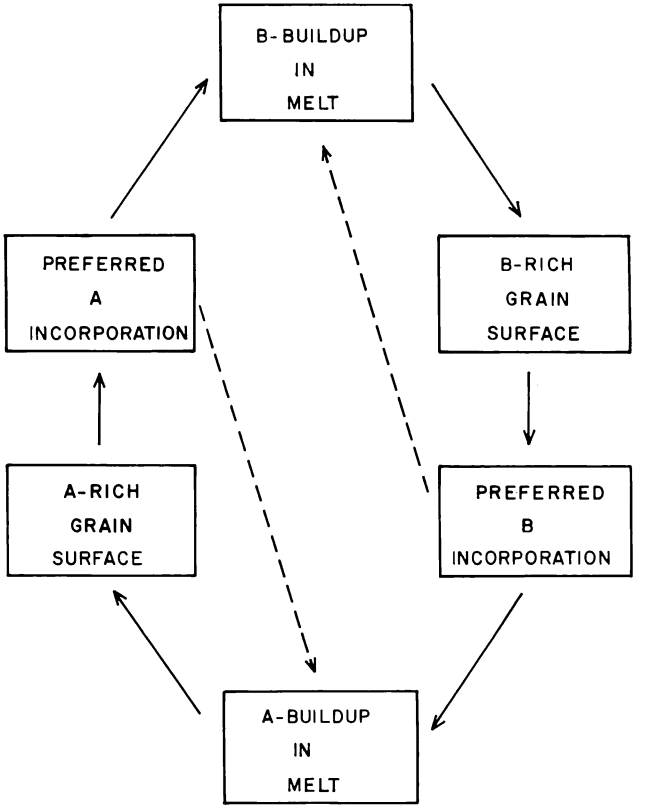

Fig. 5. Coupling between grain growth and melt diffusion for the development of periodic zoning in a binary solid solution grain. The essence of this patterning is that grain growth is surface-attachment limited (and not diffusion limited) and that it is autocatalytic for one or both components (A, B), that is, a B-rich crystal surface incorporates B ions from the melt in preference to A ions. Solid arrows indicate a promoting relation between two boxed items; the dashed arrows indicate that the boxed item emitting the arrow works against the target box.

1. Texture-pressure solution coupling.—When a rock is under overall stress, a given grain experiences a stress that is related in a complex way to the shape, mineral type, packing, and orientation of the grains around it. In an averaged way, therefore, the state of stress of a given grain depends on the local texture. Because the free energy of a solid depends on its state of stress, we can view a grain in a stressed rock as having an equilibrium constant that depends on local texture. In particular, for a stiff mineral in a rock under stress, the higher the mineral's mode at a point the less the stress borne by each grain, and the lower its solubility there. Thus, we may assume that the equilibrium constant depends on local mode (volume fraction) of each mineral and on porosity (volume fraction of the rock that is pore space).

Consider a rock containing minerals A and B and a pore fluid. For simplicity take B to be insoluble in the pore fluid and assume the porosity to be negligible. Suppose A is stiffer than B, and suppose there is sufficient A to support the rock if B were not present. Then the overall stress tends to be borne by A and hence the higher the local mode of A, the lower the free energy of each A-grain. Consequently, neighboring regions with different modes of A will, by diffusion, exchange solutes involved in the dissolution of A, because A grains will grow in regions of higher A mode at the expense of dissolving A grains in regions of lower A mode. This feedback, illustrated by the loop of figure 6, can explain spontaneous and regular metamorphic differentiation and has been quantitatively studied by Ortoleva, Merino, and Strickholm (1982) and Stickholm, Ortoleva, and Merino (unpub. ms).

Another texture-pressure solution feedback, similar to the one discussed in the previous paragraph, can also work in rocks with considerable porosities (say, >0.05). Here, the porosity itself is the key variable: a local porosity larger in one small region than in neighboring ones can result in increased local stress and hence increased local free

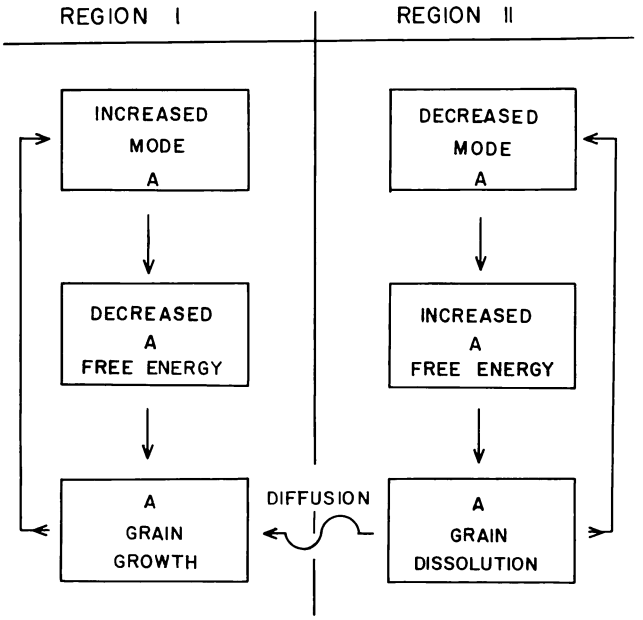

Fig. 6. Texture-solubility feedback that can lead to metamorphic differentiation. If the free energy of an A grain decreases with increasing local mode of A when the rock is under overall stress, then the indicated runaway loop can be operative. The wavy arrow indicates diffusive transfer of material between spatial regions I and II; it is this diffusion that couples A-dissolution in region II to A-growth in region I, completing the overall feedback loop.

energy. This drives local grain dissolution and loss of resultant product solutes through diffusion to neighboring, lower-free-energy regions having lower porosity. The concomitant increase of porosity in the initially higher porosity region completes this positive feedback loop. This was the feedback system used by Merino, Ortoleva, and Strickholm (1983) to account for stylolites. Porous rocks under applied compressional stress also tend to compact—that is, lose porosity—via pressure solution leading to grain flattening and plastic deformation. Thus, compaction clearly opposes the above feedback loop and may shut it off. Self-organization in this case is a balance between compaction and the porosity-solubility feedback mechanism.

The metamorphic layering and stylolitization feedback loops are analogous. Porosity plays the same role as the more compliant mineral B in the A, B model discussed above.

2. Defect density-solubility coupling.—Grain solubility increases also with increasing defect density (see citations in Wintsch and Dunning, 1985). A 'defective' grain in a rock under stress-softening conditions is more compliant than non-defective ones and therefore places a larger burden on neighboring grains to sustain the local overall average stress. This additional stress increases the free energy of these neighbors and, in addition, may create defects in them (for example, Nicolas and Poirier, 1976) and render them more soluble. Meanwhile, the original defective grain will dissolve, placing further stress on its neighbors along the direction transverse to the applied stress. These, in turn, also commence to dissolve preferentially, because of the combined increase in free energy caused by pressure solution and defect density. These processes could continue until all grains dissolve along a plane perpendicular to the applied stress spreading out from the original 'defective' grain. This puts additional stress on the original grain producing more defects in it and completing the feedback loop. Clearly this can be a mechanism of stylolite formation in essentially porosity free rocks and explains how an initially point-like textural heterogeneity could become a planar feature such as a stylolite. This mechanism seems to us more realistic and plausible than the interesting idea proposed by Fletcher and Pollard (1981) of regarding stylolites as anti-cracks.

3. Complex multiply-coupled behavior.—These feedbacks between solubility and either mode, porosity, or defect density may interact with each other and play an active role in complex mechano-chemical feedback loops in stressed rocks. This complex feedback could generate self-organization into patterns in several textural variables on multiple length scales.

E. Competitive Particle Growth (CPG)

Because of surface tension, the free energy per unit mass of a spherical precipitate particle increases with decreasing radius. Because of this, a particle can grow at the expense of its smaller neighbors by consuming dissolution-product solutes whose flux is driven to the larger

particle by the higher solubility of the smaller one. This leads to Ostwald ripening whereby a sol evolves to states of fewer but larger particles (Lifshitz and Slyozov, 1961). This competitive particle growth (CPG) mechanism can also act collectively to form macroscopic patterns (Feeney and others, 1983; Ortoleva, 1984a, b).

The feedback loop of figure 6 may be interpreted as applying to the evolution of a precipitate if the local mode of A is replaced by the local average particle radius. Thus if particles in region I were on the average larger than those in region II (see fig. 6) then the former would grow at the expense of the latter via the CPG mechanism. This model has been used to explain the spontaneous generation of precipitate patterns in laboratory (Feeney and others, 1983; Ortoleva, 1984a, b) and geological (Boudreau, 1984) systems.

F. Thermal Feedback

For completeness it is important to note that self-organization can also occur when a temperature gradient is applied to a non-reacting porous medium. The resulting thermally-induced buoyancy-driven flows have been studied extensively in the literature and will not be further discussed here, because our emphasis is on self-organization phenomena involving chemical reaction. However, if thermal effects are coupled to the above mechanism new self-organization phenomena should become possible.

G. Summary of Sections I–III

We have just described several feedbacks. In section II we listed numerous descriptive variables that can interact through various combinations of processes. There exists also much experimental evidence of chemical self-organization (see, for example, Field and Burger, 1985; and the review by Stern, 1967). In the Introduction we have summarized a number of petrological textures and occurrences whose explanation requires feedback and self-organization. All these reasons strongly warrant regarding geochemical self-organization as an inevitable and widespread phenomenon in rocks of all types and as one that directly reveals the complex dynamics of geochemical systems.

The study of geochemical self-organization in a given system could start by identifying the relevant descriptive variables and likely processes involved in its evolution. Next, one should devise working feedback loops, and one should establish that the system is out of equilibrium. For this, at least one of the mechanisms participating in the feedback must be driven out of equilibrium. The following step would be to model the feedback quantitatively (following the guidelines discussed in section IV below, for example) and, furthermore, to identify textures and occurrences in the system of interest *that cannot be inherited.* Correct models should predict time and length scales of patterning in agreement with those observed.

It is common to use diagrams to characterize domains of behavior of a physical system in terms of a set of "control" parameters. Phase diagrams and deformation maps are familiar examples. Diagrams are also useful in organizing results on the analysis of nonequilibrium systems.

Consider a water-rock system consisting of an aquifer with imposed flow. One goal of modeling this system would be to delineate the domains in system parameter space in which various phenomena may occur. Control parameters in this case are the inlet fluid velocity and composition and the initial mineralogy. From the feedback loops of subsections III.A.1 and 2 we see that at least two types of self-organization feedback loops exist in a water-rock system: the reactive-infiltration instability and the supersaturation-nucleation-depletion loop. These two feedbacks and others may produce a rich variety of self-organized patterns, such as

- dissolution fingering or scalloping of reaction fronts,
- repeated (or repetitive) precipitation in bands, spots, or other two- or three-dimensional precipitate patterns,
- multiple interacting mineral banding,
- mixed fingering and banding phenomena.

Each pattern would be represented by a field in terms of appropriate control variables on a nonequilibrium behavior diagram. This list could be extended, when it is recognized, from experience on other nonequilibrium reaction-transport systems, that there can be chaotic as well as periodic dynamical behavior and hence the possibility of generating irregularly spaced bands.

In nonequilibrium systems there can be more than one physically realizable (that is, stable) state of the system for a given domain of control parameter values (Nicolis and Prigogine, 1977). In such a case the particular pattern attained depends on initial data or the statistics of the noise the system experiences. Thus nonequilibrium behavior diagrams can be much more complex than equilibrium phase diagrams. These self-organization maps should constitute good tools to systematize quantitative experimental or theoretical studies on the self-organization of a system. For the case of metamorphic banding we have obtained (Strickholm, Ortoleva, and Merino, ms) the nonequilibrium behavior diagram shown in figure 7.

IV. MODELING OF WATER-ROCK INTERACTION

In sections III.A.1 and 2 we have discussed two types of reaction-transport feedback to expect in water-rock interaction systems. The dynamics of these two feedbacks and the self-organization patterns caused by each will be studied in detail in articles to follow the present one. Here we present the basis of the modeling approach we will use (Ortoleva and others, 1986b) focusing in particular on a few conceptual and computational insights that make the model able to yield predictions of water-rock mass transfer over geologically realistic length and time

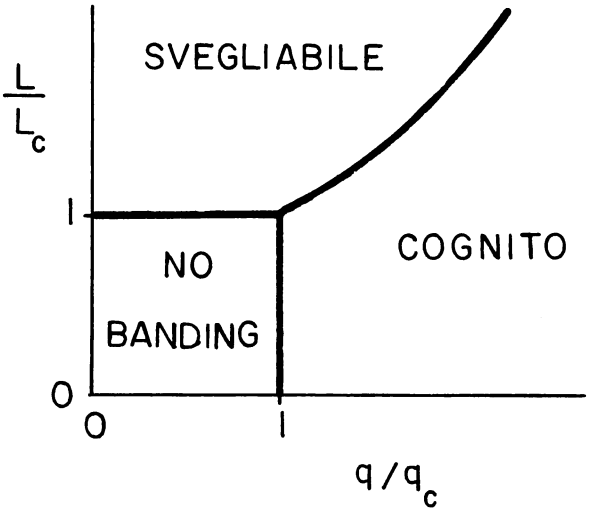

Fig. 7. Example of a nonequilibrium behavior diagram, here for differentiated layering produced by coupled grain-boundary diffusion and grain dissolution/growth in a bimineralic rock subjected to an overall stress (Strickholm, Ortoleva, and Merino, ms.) The map shows three regions in terms of the texture of the initial, unbanded rock: one in which "svegliabile" banding takes place, another in which "cognito" banding takes place, and a third in which the rock does not become banded. The coordinates are: (L/L_c), where L is the ratio of average sizes of grains of the two minerals, and L_c is a critical value of this ratio; and (q/q_c), where q is the ratio of modal amounts of the two minerals and q_c is a critical value of this ratio. In "cognito" banding, by definition, among all the patterns that exist in the textural noise present initially in the rock, there is one that under stress grows faster than the others and becomes dominant. By "svegliabile" self-organization we mean the system is triggered into becoming banded by macroscopic applied overall gradients or by certain boundary conditions.

scales. These predictions can be carried out with the program REACTRAN, which incorporates space and time, diffusion and flow, rates for homogeneous and heterogeneous reactions, reaction-transport feedback, rock textural variables, and asymptotic analytical methods. Existing programs of the PATHCALC type (for example, Helgeson, 1968; Fritz, 1981; Reed, 1982; Wolery, 1984) do not contain these features.

A. Multiple Scales in Water-Rock Systems

In the study of water-rock interactions it is highly useful to recognize that they often occur on *multiple scales* of time, length, and/or concentration, and that there exist in such cases dimensionless parameters (= ratios of characteristic times, lengths, or concentrations entering the problem) which have very small values. These small values are at once (A) responsible for the difficulty one encounters in performing geologically realistic numerical simulations of water-rock interaction and (B) at the very basis of the modeling method we propose below. For

example, if we are interested in the generation of a textural pattern, which evolves via slow mineralogical reactions having a long characteristic time, t_1, and if t_2 is the time scale of processes (such as most homogeneous aqueous reactions) much faster than the textural patterning of interest, and if we carry out a proper nondimensionalization of the reaction-transport equations (see below), then the samll parameter $\epsilon = t_2/t_1$ can be made to appear explicitly in these equations. The core of our modeling approach is to solve these equations asymptotically, that is, for the limit $\epsilon \rightarrow 0$. As shown below, this procedure self-consistently (A) focuses the calculation on reaction and transport processes having a time scale relevant to the process of interest (for instance, the mineal patterning phenomenon); (B) eliminates processes on irrelevant scales (that is, much faster or much slower than that of interest); and (C) allows us to carry out numerical calculations of reaction and transport over geologically significant times and lengths. In short, it is the very multiplicity of scales embedded in the dynamics of reaction-transport problems that allows us to solve them.

B. Basic Assumptions of the Modeling Approach

In our modeling approach we assume the following:

1. The intergranular fluid completely fills the pores and is incompressible, and its density and viscosity do not change appreciably with solute content.
2. The intergranular fluid flow obeys Darcy's law; the permeability is regarded as a function of the local texture.
3. The rate of mineral growth/dissolution is limited by surface attachment.
4. The solutes are transported by advection, diffusion, and dispersion.
5. Solute concentrations in the fluid phase are very small relative to mineral densities.
6. Some aqueous-phase reactions are extremely fast.

We demonstrate that assumptions 5 and 6, certainly valid in most water-rock systems, place strong limitations on the types of solutions that the mass conservation equations yield.

C. Conservation of Mass

The fundamental equation of mass conservation is for example, DeGroot and Mazur, 1962):

$$\begin{bmatrix}\text{Rate of change}\\ \text{of mass of species}\\ \text{i in } \Delta V\end{bmatrix} = \begin{bmatrix}\text{Next rate of}\\ \text{influx of i}\\ \text{into } \Delta V\end{bmatrix} + \begin{bmatrix}\text{Net rate of change}\\ \text{of mass of i in } \Delta V\\ \text{caused by reactions}\end{bmatrix} \qquad \text{(IV.1)}$$

where ΔV is a small volume element of the system large enough to contain many mineral grains. It must be small enough, however, that $\Delta V^{1/3}$ is less than the typical length scale of the pattern or phenomena to

be described. Also, (IV.1) relates transport and reactions, thus constituting a perfect framework to explore reaction-transport feedbacks.

Let c_i be the concentration (moles/pore fluid volume) of solute species i, and ϕ be the porosity (volume fraction of rock occupied by pore space). The general equation (IV.1) can now be written for the concentration of i (per unit of *rock* volume), ϕc_i, as

$$\frac{\partial \phi c_i}{\partial t} = -\vec{\nabla} \cdot \vec{J}_i + \phi R_i + \sum_{\alpha=1}^{N_m} \nu_{i\alpha} n_\alpha \rho_\alpha \frac{\partial V_\alpha}{\partial t} \qquad \text{(IV.1A)}$$

where

$\vec{J}_i$ = flux of species i (moles/sec × cm^2 of rock cross section)
$\vec{\nabla} \cdot \vec{J}_i$ = net rate of change of ϕc_i due to transport
ϕR_i = net rate of change of ϕc_i due to aqueous reactions
$\nu_{i\alpha}$ = stoichiometric coefficients for solute i due to dissolution or precipitation of mineral α
n_α = number of α grains per rock volume
V_α = volume of a grain of mineral α
ρ_α = molar density of mineral α (moles/cm^3)
N_m = number of mineral species.

The last term in (IV.1), which is the reaction term, has been broken down into the last two terms of (IV.1A), which respectively represent the contribution of homogeneous aqueous reactions and the contributions of the reactions of mineral dissolution or growth.

The net rate, R_i, of aqueous reactions affecting species i can be written in an expanded form to emphasize that some of these processes often take place on time scales much shorter than that of interest in the development of textural patterns. Assume there are N_f fast aqueous reactions. Let W_β/ϵ denote the rate of the β-th of the N_f fast reactions. $\beta = 1, 2, \ldots N_f$. Here, W_β depends on pore fluid composition; the smallness parameter ϵ explicitly emphasizes that the N_f reactions are fast, because $\epsilon \ll 1$. Recall that ϵ represents the ratio of the time for a *fast* reaction to come to equilibrium divided by a typical time for the development of a textural pattern. With this we separate R_i into two contributions as follows:

$$R_i = \sum_{\beta=1}^{N_f} \omega_{i\beta} \frac{W_\beta}{\epsilon} + R_i' \qquad \text{(IV.2)}$$

where R_i' is the remaining contribution to R_i from *slow* aqueous reactions, and $\omega_{i\beta}$ is a stoichiometric coefficient for aqueous species i in the *β-th* fast aqueous reaction. Combining IV.1A and IV.2 we obtain an equation of motion of c_i which can be analyzed in the limit $\epsilon \to 0$ to account explicitly for both fast equilibria and slower processes as discussed in section E below.

We now explicitly introduce in the equation of mass conservation the fact that mineral densities normally are *orders of magnitude* greater than typical aqueous concentration (assumption 5 above). If $\bar{c}$ denotes a

typical value of a solute concentration and ρ a typical solid molar density, then

$$\delta \equiv \bar{c}/\rho \ll 1. \tag{IV.3}$$

(For example, $\bar{c} = c^{sat}$ for quartz, $\delta \sim 10^{-6}$.) Defining a new dimensionless, order-one, concentration of i by

$$\gamma_i \equiv c_i/\bar{c} \tag{IV.4}$$

we obtain from (IV.1A)

$$\frac{\partial \phi \gamma_i}{\partial t} = -\vec{\nabla} \cdot \vec{j}_i + \phi r_i + \phi \sum_{\beta=1}^{N_f} \omega_{i\beta} \frac{w_\beta}{\epsilon} + \sum_{\alpha=1}^{N_m} \frac{\nu_{i\alpha} n_\alpha}{\delta} \hat{\rho}_\alpha \frac{\partial V_\alpha}{\partial t} \tag{IV.5}$$

where,

$$\begin{aligned} \hat{\rho} &\equiv \rho_\alpha/\rho \\ r_i &\equiv R_i'/\bar{c} \\ \vec{j}_i &\equiv \vec{J}_i/\bar{c} \\ w_\beta &\equiv W_\beta/\bar{c}. \end{aligned} \tag{IV.6}$$

In this version of the continuity equation it becomes clear why straightforward numerical solution of the solute equations is impractical: ϵ and δ can each be $10^{-3} - 10^{-12}$ and cause the last two terms in (IV.5) to become enormous. Under these conditions a numerical integration of (IV.5) would require huge computer times to simulate systems on length and time scales of geological interest. But at the same time this very "stiffness" of the problem opens the possibility of carrying out certain simplifications and improvements in the calculations. This turns us to the asymptotic ($\epsilon, \delta \to 0$) analysis of the solute equations, discussed in section E and F below.

D. Other Phenomenological Relations

The physics of a given situation dictates the phenomenological dependence of the homogeneous-reaction rates r_i and w_β, the flux $\vec{j}_i$, and the growth rate $\partial V_\alpha/\partial t$ on the descriptive variables $\{V_\alpha, \gamma_i\}$; V_α is the volume of a grain of mineral α, and γ_i is the dimensionless concentration of aqueous species i, defined in (IV.4). Typical general forms are as follows:

$$r_i = r_i(\gamma) \tag{IV.7}$$

$$w_\beta = q_\beta F_\beta(\gamma) \tag{IV.8}$$

$$\frac{\partial V_\alpha}{\partial t} = k_\alpha E_\alpha(\gamma) \tag{IV.9}$$

$$\vec{j}_i = -\phi D_i \vec{\nabla} \gamma_i + \phi \gamma_i \vec{v} \tag{IV.10}$$

$$\vec{v} = -\kappa \vec{\nabla} p \text{ (Darcy's law)} \tag{IV.11}$$

where

$\gamma = \{\gamma_1, \gamma_2, \ldots \gamma_N\}$
q_β = rate constant for fast aqueous reaction β
k_α = rate constant for the growth of mineral α; for surface attachment limited kinetics, k_α is proportional to the surface area of an α grain.
D_i = effective diffusion coefficient of species i
$\vec{v}$ = flow velocity of the aqueous fluid
κ = permeability divided by the viscosity of the pore fluid
p = pressure

The function $r_i(\gamma)$ yields the overall rate of the slow aqueous reactions contributing to aqueous species i. When fast reaction β is at equilibrium the function F_β vanishes, yielding the equilibrium relations among the scaled concentrations. When F_α vanishes the fluid composition is at equilibrium with respect to mineral α. The specific forms of these functions are not of interest here. The flux $\vec{j}_i$ involves the advective contribution $\phi\gamma_i\vec{v}$, where $\vec{v}$ is given by Darcy's law (IV.11), where the permeability divided by the viscosity, κ, can depend on texture: that is, $\kappa = \kappa(\phi, V_1, V_2, \ldots V_{N_m}, n_1, n_2, \ldots n_{N_m})$, where n_α is the grain number density or number of grains of mineral α per unit volume of rock. The D_i contribution to $\vec{j}_i$ accounts for diffusion and dispersion. D_i depends on texture and, because of dispersion, on velocity $\vec{v}$.

An equation for the pressure follows from conservation of water. Let ρ_w be the molar density of water. Then conservation of water for a medium with filled pores can be written (letting R_w be the net rate of production of H_2O from all processes)

$$\frac{\partial \phi \rho_w}{\partial t} = -\vec{\nabla} \cdot (\phi \rho_w \vec{v}) + R_w. \tag{IV.12}$$

Because ρ_w is taken to be constant by assumption 1, this equation yields, using Darcy's law (IV.11),

$$\frac{\partial \phi}{\partial t} = \vec{\nabla} \cdot [\phi \kappa \vec{\nabla} p] + R_w/\rho_w. \tag{IV.13}$$

Our description is completed via the relation

$$\phi + \sum_{\alpha=1}^{N_m} n_\alpha V_\alpha = 1 \tag{IV.14}$$

stating that the entire volume of the rock is either pore space or is filled by mineral grains, $n_\alpha V_\alpha$ being the volume fraction (or mode) occupied by mineral α.

Eqs (IV.7–14), together with the continuity equation in its form (IV.5), yield quantitatively the dynamics of the evolution of reaction-transport feedbacks in water-rock systems. We will use detailed versions of these equations in the articles to follow the present one. Note now

that the equations link textural and fluid composition variables and the advection velocity.

E. Fast Aqueous-Reaction Asymptotics ($\epsilon \rightarrow 0$)

We study here the limit of our descriptive eqs (IV.5, 7–11, 13, 14) as $\epsilon \rightarrow 0$, that is, when the fast reactions in the aqueous phase occur on a time scale much shorter than that of mineral pattern formation. Under these conditions the "well-behaved" solutions of (IV.5) must be such that the w_β also become zero: only in this way can the rates w_β/ϵ have finite values. Hence, by eq (IV.8) as $\epsilon \rightarrow 0$ the scaled concentrations, γ_i, must satisfy the N_f eqs $F_\beta(\gamma) = 0$ where γ is the vector of the N γ_i concentrations. We choose to solve these equations for the first N_f γ_i's as a function of the remaining $(N - N_f)$ concentrations, which we now denote by b_k to distinguish them from the first N_f concentrations. The first N_f concentrations will then be

$$\gamma_i = \Gamma_i(b),\ i = 1, 2, \ldots N_f \tag{IV.15}$$

where the vector b consists of the components

$$b_k = \gamma_{N_f+k},\ k = 1, 2 \ldots N_b (\equiv N - N_f). \tag{IV.16}$$

The most convenient choice is to take as b_k's the concentrations in terms of which it is easiest to express the other N_f concentrations.

Now comes the main step of the development—to obtain a system of equations for the b_k's which are "well-behaved" as $\epsilon \rightarrow 0$. For this, first solve algebraically the mass conservation eq (IV.5) for the N_f rates w_1/ϵ, w_2/ϵ, $\ldots$ w_{N_f}/ϵ. Then insert these w/ϵ's into the remaining N_b (IV.5) equations, that is, for $i = N_f + 1, N_f + 2, \ldots N$. The result is a set of $(N - N_f)$ equations of the form

$$\frac{\partial \phi b'_k}{\partial t} = -\vec{\nabla} \cdot \vec{J}^{\,b}_k + r^b_k(b) + \sum_{\alpha=1}^{N_m} \nu^b_{k\alpha}\ \delta^{-1}\, n_\alpha \hat{\rho}_\alpha \frac{\partial V_\alpha}{\partial t} \tag{IV.17}$$

$$b'_k = b_k - \sum_{i=1}^{N_f} \lambda_{ki}\, \Gamma_i(b) \tag{IV.18}$$

where the $\nu^b_{k\alpha}$ are stoichiometric-like coefficients, and the r^b_k are linear combinations of the scaled rates of the slow reactions, r_i. The coefficients λ_{ki} are related to the stoichiometric coefficients $\omega_{i\beta}$ of (IV.5). The b-flux in the transport term is given by

$$\vec{J}^{\,b}_k = \vec{J}_{N_f+k} - \sum_{i=1}^{N_i} \lambda_{ki}\, \vec{J}_i \tag{IV.19}$$

where, by (IV.15), γ_i has been replaced by $\Gamma_i(b)$ in obtaining (IV.17, 18). Eq (IV.17) is an important result: It yields the dynamics of the system in a way consistent with the fast aqueous reactions while correctly retaining the finite rate of the slower aqueous and mineral reactions and transport. These equations, which yield the values of all relevant variables as

functions of time *and* space, will find application in modeling the reactive infiltration instability and the supersaturation-nucleation-depletion feedback, which will appear in forthcoming articles.

F. Solid-Density Asymptotics ($\delta \to 0$)

The smallness of the ratio δ of a typical aqueous species concentration to a typical mineral density causes the time scale of mineral dissolution or precipitation to be long. This suggests defining a scaled time τ such that

$$\tau = \delta t. \tag{IV.20}$$

With this (IV.13, 17) become

$$\delta \frac{\partial \phi}{\partial t} = \vec{\nabla} \cdot (\phi \kappa \vec{\nabla} p) + R_w/\rho_w \tag{IV.21}$$

$$\delta \frac{\partial \phi b'_k}{\partial \tau} = -\vec{\nabla} \cdot \vec{j}^{\,b}_k + \phi r^b_k(b) + \sum_{\alpha=1}^{N_m} \nu^b_{k\alpha} n_\alpha \hat{\rho}_\alpha \frac{\partial V_\alpha}{\partial \tau} \tag{IV.22}$$

Clearly, as $\delta \to 0$ the left-hand side terms in (IV.21, 22) become zero; in other words, the two equations take their steady state forms

$$\vec{\nabla} \cdot [\phi \kappa \vec{\nabla} p] = 0 \tag{IV.23}$$

$$-\frac{1}{\phi} \vec{\nabla} \cdot \vec{j}^{\,b}_k + r^b_k(b) + \sum_{\alpha=1}^{N_m} \nu^b_{k\alpha} n_\alpha \hat{\rho}_\alpha \frac{\partial V_\alpha}{\partial \tau} = 0. \tag{IV.24}$$

In (IV.23) we have dropped the R_w term, because it involves production rates of order of a typical mobile species concentration $\bar{c}$ divided by a characteristic time and by ρ_w, and $\bar{c}/\rho_w$ is also of order δ. Finally, (IV.24) states that the b concentration—see (IV.16)—is governed by a steady-state balance between transport and the *slow* aqueous and mineral reactions.

To complete this general discussion of the solid-density asymptotics we must distinguish between fast and slow mineral reactions. First we rewrite (IV.9) making it explicit that $\partial V_\alpha/\partial t$, the rate of dissolution or growth of an α grain, is proportional to the surface area of the grain, which is proportional to $V_\alpha^{2/3}$:

$$\partial V_\alpha/\partial t = k_\alpha E(\gamma) = \tilde{k}_\alpha V_\alpha^{2/3} E(\gamma), \tag{IV.25}$$

and now we insert the new time τ defined in (IV. 20):

$$\delta(\partial V_\alpha/\partial \tau) = \tilde{k}_\alpha V_\alpha^{2/3} E(\gamma). \tag{IV.25A}$$

As $\delta \to 0$, the left side $\to 0$. Two general cases arise.

1. For *fast* reactions (that is, reactions with a large $\tilde{k}_\alpha$), for the right side to tend to zero, either $E(\gamma) = 0$ or $V_\alpha = 0$. The case $E(\gamma) = 0$ implies that the pore fluid is in equilibrium with mineral α; the case $V_\alpha = 0$

means that there is no mineral α. Thus for fast reactions space is divded into regions devoid of α and regions where the pore fluid is constrained to be in equilibrium with it. The two types of regions are separated by interfaces, or fronts, across which V_α changes discontinuously as $\delta \rightarrow 0$; the movement of these interfaces is governed by discontinuity relations among the normal derivatives of the aqueous-species concentrations, as discussed in Auchmuty and others (1985) and Ortoleva and others (1986a).

2. For reactions *slow enough* that $\tilde{k}_\alpha$ itself becomes of order δ we can write

$$\tilde{k}_\alpha = \delta k'_\alpha \qquad \text{(IV.25B)}$$

and then (IV.25A) becomes

$$\delta(\partial V_\alpha/\partial \tau) = \delta k'_\alpha \, V_\alpha^{2/3} \, E(\gamma). \qquad \text{(IV.26)}$$

After cancelling the δ's, this equation, together with (IV.23, 24), shows that, for slow reactions, the α-grain volume must change gradationally in space. Thus, in contrast to the fast-reaction case the reaction zone has non-zero thickness as $\delta \rightarrow 0$.

The relevance of these general considerations is supported by the existence in rocks of sharp as well as gradational modal variations for one or another mineral or assemblage. Examples of these are the zones around concretions (Berner, 1980; Fisher, 1970, and references therein) or behind redox fronts (Bailey and Childers, 1977), or skarn mineral bands (for example, Joesten, 1974); all these cases involve flow and/or diffusion of aqueous solutions during the genesis of the textures and structures cited.

SUMMARY AND CONCLUSIONS

Disequilibrium can create mineralogical or textural patterns in geochemical systems in which reaction and transport operate and interact; the process is termed geochemical self-organization, and it should be widespread in rocks because both reaction-transport feedbacks and disequilibrium are the rule rather than the exception in geochemical systems. Indeed, rocks of all kinds can display a number of mineralogical or textural patterns that are *not* inherited and must therefore result from some type of spontaneous self-organization. Criteria to establish that a given textural or mineralogical or chemical pattern is indeed non-inherited vary depending on the specific pattern at hand and in general include field, petrographic, and chemical considerations. Many examples are given and referenced in the text.

The generation of a self-organization pattern comes about when a given feedback is triggered by noise and driven by disequilibrium. Only isothermal reaction-mass transport feedbacks are considered here for

simplicity; the possibilities for self-organization increase vastly if the feedbacks include energy transfer. The operation of the following feedbacks is studied qualitatively and in detail:

1. Where reactive water flows through a rock, at points where the porosity is initially higher than elsewhere the local flux of reactive water is also higher than elsewhere, and so the local dissolution rate becomes higher; this in turn makes the local porosity and permeability even greater. This *reactive infiltration instability* should cause reaction fronts to become fingered or scalloped.

2. In the supersaturation–nucleation–depletion cycle, as a reaction front sweeps through a rock and causes supersaturation of the fluid at a point A with respect to a given mineral, nucleation and growth of the mineral take place at A but cannot happen again until the front travels far enough downflow from A, because the mineral precipitated at A precludes further nucleation in its neighborhood by consuming coprecipitates. This instability can give rise to evenly spaced bands of authigenic cements (bands that may also become scalloped by the reactive infiltration instability).

3. In the growth of an (A, B) solid solution crystal from a melt, if the attachment of A ions onto a A-rich crystal surface happens to be favored by geometric or other factors and happens to be fast enough, then the melt around the growing crystal eventually becomes depleted enough in A and concentrated enough in B to force growth B layers. If the attachment of B ions on B-rich layers is also autocatalytic the crystal develops oscillatory zoning.

4. In rocks subjected to an overall deviatoric stress several feedbacks are possible, because the solubility of each mineral grain depends on its state of stress, which depends on the local texture around the grain, and because, in turn, the grain's dissolution or growth modifies that very texture. These texture-solubility feedbacks can account for the generation of differentiated layering in regionally metamorphosed rocks and evenly spaced stylolites in porous and only slighty porous sedimentary rocks.

5. Competitive particle growth allows for larger grains in one region of space to grow at the expense of smaller ones in another, because the free energy of a grain is a decreasing function of its radius due to surface tension. Thus when diffusion interacts with competitive particle growth, nonuniformities in the spatial distribution of particle size become accentuated.

A new general modeling approach is proposed here to calculate the evolution of disequilibrium reaction-transport systems. The approach takes account of reaction-transport feedbacks, is based on the continuity equation, and, by means of scaling and asymptotic analysis, permits numerical solutions of the system's evolution as functions of time and space to be carried out over geologically significant times and distances (that is, up to millions of years and hundreds of meters).

ACKNOWLEDGMENTS

The authors greatly appreciate the many thoughtful suggestions of the referees.

REFERENCES

Auchmuty, G., Chadam, J., Merino, E., Ripley, E., and Ortoleva, P., 1985, The stability and structure of moving redox fronts: Soc. Indus. Appl. Math, Jour. Appl. Math.

Bailey, R. V., and Childers, M. O., 1977, Applied Mineral Exploration with Special Reference to Uranium: Boulder, Colo., Westview Press, 542 p.

Barret, P. J., 1964, Residual seams and cementation in oligocen shell calcarenites, Te Kuiti Group: Jour. Sed. Pet., v. 34, p. 524–531.

Beales, F. W., and Hardy, J. L., 1980, Criteria for the recognition of diverse dolomite types with an emphasis on studies on host rocks for Mississippi Valley-type ore deposits, *in* Zenger, D. H., Dunham, J. B., and Ethington, R. L., eds., Concepts and Models of Dolomitization: Soc. Econ. Paleontologists Mineralogists, Spec. Pub. 28, p. 197-213.

Berner, R. A., 1980, Early Diagenesis: Princeton, N. J., Princeton Univ. Press, 241 p.

Boeglin, J. B., ms, 1981, Mineralogie et geochimie des gisements de manganese de Conselheiro Lafaiete au Bresil et de Moanda au Gabon: These Doctorat 3 eme. Cycle, Univ. Toulouse, 155 p.

Boudreau, A. E., 1984, Examples of patterns in igneous rocks, *in* Nicolis, G., and Baras, F., eds., Chemical Instabilities—Applications in Chemistry, Engineering, Geology and Materials Science: Dordrecht, Reidel, NATO Adv. Sci., ser. C, v. 120, p. 299–304.

Boulange, B., ms, 1983, Les mecanismes de la bauxitisation lateritique en zone tropicale (Cote d'Ivoire): Doctoral thesis, Univ. Paris VII, 280 p.

DeCelles, P. G., and Gutschick, R. C., 1983, Mississippian woodgrained chert and its significance in the western interior, United States: Jour. Sed. Pet., v. 53, p. 1175–1191.

DeGroot, S. R., and Mazur, P., 1962, Non-equilibrium Thermodynamics: Amsterdam, North-Holland, 510 p.

Downes, M. J., 1974, Sector and oscillatory zoning in calcic augites from Mt. Etna, Sicily: Contr. Mineralogy Petrology, v. 47, p. 187–196.

Dunnington, H. V., 1967, Aspects of diagenesis and shape change in stylolitic limestone reservoirs: World Petroleum Cong., 7th, Mexico, Proc., v. 2, p. 339–352.

Feeney, R., Schmidt, S. L., Strickholm, P., Chadam, J., and Ortoleva, P., 1983, Periodic precipitation and coarsening waves: applications of the competitive particle growth model: Jour. Chemistry Physics, v. 78, p. 1293–1311.

Field, R. J., and Burger, M., 1985, Oscillations and Travelling Waves in Chemical Systems: Park Ridge, Ill., Wiley, 688 p.

Fisher, G. W., 1970, The application of ionic equilibrium to metamorphic differentiation: an example: Contr. Mineralogy Petrology, v. 29, p. 91–103.

Fletcher, R. C., and Pollard, D. D., 1981, Anticrack model for pressure solution surfaces: Geology, v. 9, p. 419–424.

Fontbote, L., and Amstutz, G. C., 1982, Observations on ore rhythmites of the Trzebionka Mine, Upper Silesian-Cracow region, Poland, *in* Amstutz G.C., and others, eds., Ore Genesis—The State of the Art: Heidelberg, Springer Verlag p. 83–91.

Fritz, B., 1981, Etude thermodynamicque et modelisation des reactions hydrothermales et diagenetiques: Sci. Geol. Mem., v. 65, 197 p.

Frondel, C., 1978, Characters of quartz fibers: Am. Mineralogist, v. 63, p. 17–27.

———— 1982, Structural hydroxyl in chalcedony (type β quartz): Am. Mineralogist, v. 67, p. 1248–1257.

———— 1985, Systematic compositional zoning in the quartz fibers of agates: Am. Mineralogist, v. 70, p. 975–979.

Galloway, W. E., 1978, Uranium mineralization in a coastal-plain fluvial aquifer system, Catahoula Formation, Texas: Econ. Geology, v. 73, p. 1655–1676.

Gower, S. J., Clark, A. H., and Hodgson, C. J., 1985, Tungsten-molybdenum skarn and stockwork mineralization, Mount Reed-Mount Haskin District, Northern British Columbia, Canada: Canadian Jour. Earth Sci., v. 22, p. 728–747.

Grubb, P. L. C., 1971, Silicates and their paragenesis in the Brockman Iron Formation of Wittenoom Gorge, Western Australia: Econ. Geology, v. 66, p. 281–292.

Guy, B., 1981, Certaines alternances recurrentes rencontrees dans les skarns et les structures dissipatives au sens de prigogine: un rapprochement: Acad. Sci., Paris, Comptes rendu, v. 292, p. 413–416.

Haase, C. S., Chadam, J., Feinn, D., and Ortoleva, P., 1980, Oscillatory zoning in plagioclase feldspar: Science, v. 209, p. 272–274.
Hartman, R. J., and Dickey, R. M., 1932, The Liesegang Phenomenon applied to the Lake Superior Iron Formations: Jour. Phys. Chemistry, v. 36, p. 1129–1135.
Hedges, E. S., and Myers, J. E., 1922, The Problem of Physicochemical Periodicity: New York, Longmans, 95 p.
Helgeson, H. C., 1968, Evaluation of irreversible reactions in geochemical processes involving minerals and aqueous solutions, I. thermodynamic relations: Geochim. et Cosmochim. Acta, v. 32, p. 853, 877.
Hobbs, B. E., Means, W. D., and Williams, P. F., 1976, An Outline of Structural Geology: New York, Wiley, 571 p.
Hobson, R. A., 1930, 'Zebra rock' from the East Kimberley: Royal Soc. Western Australia Jour., v. 16, p. 57–70.
Hosking, K. F. G., 1953–54, The vein system of St. Michael's Mount: Royal Geol. Soc. Cornwall Trans., v. 18, p. 493–509.
Jahns, R. H., 1944, 'Ribbon rock' an unusual beryllium-bearing tactite: Econ. Geology, v. 39, p. 173–205.
Joesten, R., 1974, Local equilibrium and metasomatic growth of zoned calc-silicate nodules from a contact aureole, Christmas Mountains, Big Bend Region, Texas: Am. Jour. Sci., v. 274, p. 876–901.
Knopf, A., 1908, Geology of the Seward Peninsula tin deposits: U.S. Geol. Survey Bull., v. 358, 71 p.
Kwak, T. A. P., and Askins, P. W., 1981, Geology and genesis of the F-Sn-W (-Be-Zn) skarn (Wrigglite) at Moina, Tasmania: Econ. Geology, v. 76, p. 439–467.
Leveson, D. J., 1966, Orbicular rocks: a review: Geol. Soc. America bull., v. 77, p. 409–426.
Liesegang, R. E., 1913, Geologische Diffusionen: Dresden and Leipzig, Steinkopff, 180 p.
———— 1915, Die Achate: Dresden and Leipzig, Steinkopff, 118 p.
Lifshitz, I. M., and Slyozov, V. V., 1961, The kinetics of precipitation from supersaturated solid solutions: Jour. Physics Chemistry Solids, v. 19, p. 35–50.
McBirney, A. R., and Noyes, R. M., 1979, Crystallization and layering of the skaergaard intrusion: Jour. Petrology, v. 20, p. 487–554.
Mel'nik, Y. P., 1982, Precambrian Banded Iron Formations: Developments in Precambrian Geology 5: Amsterdam, Elsevier, 310 p.
Merino, E., 1984, Survey of geochemical self-patterning phenomena, *in* Nicolis, G., and Baras, F., eds., Chemical Instabilities: Applications in Chemistry, Engineering, Geology, and Materials Science: Dordrecht, Reidel, NATO Adv. Sci. Ser. C, v. 120, p. 305–328.
Merino, E., Ortoleva, P., and Strickholm, P., 1983, Generation of evenly-sapced pressure-solution seams during (late) diagenesis: a kinetic theory: Contr. Mineralogy Petrology, v. 82, p. 360–370.
Moore, A. C., 1984, Orbicular rhythmic layering in the Palabora Carbonatite, South Africa: Geol. Mag., v. 121, p. 53–60.
Nahon, D., 1976, Cuirasses Ferrugineuses et Encroutements Calcaires au Senegal occidental et en Mauritanie. Systemes evolutifs: Geochimie, Structures, Relais et Coexistence, Strasbourg: Mem. Sci. Geol., v. 44, 232 p.
Nahon, D., Carozzi, A., and Parron, C., 1980, Lateritic weathering as a mechanism for the generation of ferroginous ovids: Jour. Sed. Pet., v. 50, 1287–1298.
Nicolas, A., and Poirier, J. P., 1976, Crystalline Plasticity and Solid-State Flow in Metamorphic Rocks: London, Wiley, 444 p.
Nicolis, G., and Prigogine, I., 1977, Self-organization in Non-equilibrium Systems: New York, Wiley, 491 p.
Ortoleva, P., 1984a, From nonlinear waves to spiral and speckle patterns: nonequilibrium phenomena in geological and biological systems, *in* Bishop, A. R., Campbell, L. J., and Channell, P. J., eds., Fronts, Interfaces and Patterns: Proc. Annual Internat. Conf. for Nonlinear Studies, 3d, Los Alamos, New Mexico, May 2–6, 1983, p. 305–320.
Ortoleva, P., 1984b, The self-organization of Leisegang Bands and other precipitate patterns, *in* Nicolis, G., and Baras, F., eds., Chemical Instabilities: Applications in Chemistry, Engineering, Geology, and Materials Science: Dordrecht, Reidel, NATO Adv. Sci. Ser. C., v. 120, p. 289–297.
Ortoleva, P., Auchmuty, G., Chadam, J., Merino, E., Hettmer, J., Moore, C., and Ripley, E., 1986a, Redox front propagation and banding modalities: Physica D, p. 334–354.
Ortoleva, P., Merino, E., and Strickholm, P., 1982, A kinetic theory of metamorphic layering in anisotropically stressed rocks: Am. Jour. Sci., v. 282, p. 617–643.

Ortoleva, P., Moore, C. H., Chadam, J., Hettmer, J., 1986b, REACTRAN USERS MANUAL, available from Geo-Chem Research Associates.
Orville, P. M., 1969, A model for metamorphic differentiation origin of thin-layered amphibolites: Am. Jour. Sci., v. 267, p. 64–86.
Parron, C., Guendon, J. L., Boulange, B., and Bocquier, G., 1983, Bauxites du Midi de la France. Evolutions Minerales et Micostructurales Mescanismes de la Gauxitisation sur Substrat Carbonate: Trav. Lab. Sci. Terre, Marseille St. Jerome, Serie X, No. 54, 51 p.
Patterson, D. J., Ohmoto, H., and Solomon, M., 1981, Geological setting and genesis of cassiterite-sulfide mineralization at Renisson Bell, Western Tasmania: Econ. Geology, v. 76, p. 393–438.
Reed, M. H., 1982, Calculation of multicomponent chemical equilibria and reaction processes in systems involving minerals, gases and an aqueous phase: Geochim. et Cosmochim. Acta, v. 46, p. 513–528.
Salomon, G., 1894, Sul Metamorphismo di Contatto Subito Dalle Arenarie Permiane Della Val Daone: Gior. Mineral. Cristallografia, Petrografia Pavia 5, p. 97–147.
Simakin, A. G., 1983, A simple quantitative model for rhythmic zoning in crystals: Geokhimiya 12, p. 1720–1729 (English translation by Scripta Publishing, 1984).
Simpson, J., 1985, Stylolite-controlled layering in an homogeneous limestone: pseudo-bedding produced by burial diagenesis: Sedimentology, v. 32, p. 495–505.
Smith, J. V., 1974, Feldspar Minerals: New York, Springer, 690 p.
Spang, J. H., Oldershaw, A. E., and Stout, M. Z., 1979, Development of cleavage in the Banff Formation at Pigeon Point Mountain, Front Ranges, Canadian Rocky Mountains: Canadian Jour. Earth Sci., v. 16, p. 1105–1115.
Stern, K. H., 1967, Bibliography of Liesegang Rings: U.S. Natl. Bur. Standards, Spec. Pub., v. 292, 61 p.
Tanelli, G., 1982, Geological setting, mineralogy and genesis of tungsten mineralization in Dayu District, Jiangxi (People's Republic of China): an outline: Mineralog. Deposita, v. 17, p. 279–294.
Tardy, Y., and Nahon, D., 1985, Geochemistry of laterites, stability of Al-goethite, Al-hematite, and Fe^{3+} kaolinite in bauxites and ferricretes: an approach to the mechanism of concretion formation: Am. Jour. Sci. v. 285, p. 865–903.
Tolok, A. A., and Fedchin, F. G., 1970, Vertical metasomatic zonality in the tin deposits of the Soviet Far East and its significance in estimating the amount of ore mineralization at depth: Internat. Geol. Rev., v. 12, p. 1191–1197.
Tremolieres, P., and Reulet, J., 1978, Influence de Deformations Tectoniques sur les Caracteristiques Petrophysiques Matricielles des Reservoirs Calcaires: Rev. Inst. Francais du Petrole, v. 33, p. 331–348.
Trendall, A. F., 1972, Revolution in Earth History: Geol. Soc. Australia Jour., v. 19, p. 287–311.
Turing, A. M., 1952, The Chemical Basis of Morphogenesis: Royal Soc. London Philos. Trans., ser. B 237, p. 37–72.
Turner, F. J., Weiss, L. E., 1963, Structural analysis of metamorphic tectonites: New York, McGraw-Hill, 545 p.
Vidale, Rosemary, 1974, Metamorphic differentiation layering in pelitic rocks of Dutchess county, New York, *in* Hoffman, A. W., and others, eds., Geochemical Transport and Kinetics: Washington, D.C., Carnegie Inst. Washington, p. 273–286.
Williams, H., Turner, F. J., and Gilbert, C. M., 1982, Petrography, 2d ed.: San Francisco, Freeman Co., 626 p.
Wintsch, R. P., and Dunning, J., 1985, The effect of dislocation density on the aqueous solubility of quartz and some geological implications: a theoretical approach: Jour. Geophys. Research, v. 90, p. 3649–3657.
Wolery, T. J., 1984, EQ6, a Computer code for reaction-path modeling of aqueous geochemical systems: Livermore, Calif., Lawrence Livermore Natl. Lab.